VALIDATION OF DIRECT CONTACT CONDENSATION CFD MODELS AGAINST CONDENSATION POOL EXPERIMENT

I1.Vesa Tanskanen, I2. Djamel Lakehal, I1. Markku Puustinen

I1,Lappeenranta University of Technology (LUT)
P.O. Box 20, FIN- 53851 Lappeenranta, Finland

I2, ASCOMP GmbH
Technoparkstrasse 1, CH-8005 Zurich, Switzerland

Abstract

An experiment related to steam discharge into sub-cooled water was carried out with a scaled down condensation pool test facility at Lappeenranta University of Technology. The vertical blowdown pipe was submerged by 1.81 m and thermally insulated. Condensation took place only at the steam-water interface near the pipe outlet. Since very low steam flow rates (1.0…1.5 g/s) were used, the steam-water interface remained steady close to the pipe outlet. Several quasi-steady intervals suitable for the validation of direct contact condensation models can be found from the experiment data. Simulations with the Hughes-Duffey based DCC model of the NEPTUNE CFD code indicated two orders of magnitude higher condensation rates than the experiment. This overestimation was reduced by one order of magnitude by decreasing the numerical truncation parameter and by disabling the residual droplet handling. By implementing the DNS-based model of Lakehal et al. (2008) the heat transfer coefficient reached the same order of magnitude as indicated by experiments. More stable transfer rate values were also attained. However, uncertainties prevail in the experimental and simulation results as the presence of non-condensables, which has a significant suppressing effect on condensation, has not been taken into account. The work was accomplished in the framework of the EU/NURESIM project.

1. INTRODUCTION

During a possible large steam line break accident inside a BWR containment a large amount of non condensable (nitrogen) and condensable (steam) gas will be blown from the upper dry well to the condensation pool through the blowdown pipes. The wet well pool serves as the major heat sink for condensation of steam.

Experiment results of the POOLEX project at Lappeenranta University of Technology (LUT) in Finland can be used for the validation of different numerical methods and models for simulating steam injection through a blowdown pipe into liquid (Tanskanen, 2008). The improvement of models is necessary for the reduction of uncertainties in predicting condensation pool behaviour during steam injection. Improvements are necessary both for the physical models (heat transfer coefficient at the interface between liquid and vapour, instabilities of the interface) and for the numerical schemes. Some of the models are applicable also outside the BWR scenarios, e.g. for the quench tank operation in the pressurizer vent line of a Pressurized Water Reactor (PWR), for the bubble condenser in a VVER-440/213 reactor system, or in case of a submerged steam generator pipe break.

EU/NURESIM project on thermal hydraulics was aimed at solving important outstanding issues, including DCC scenarios. LUT has participated in the NURESIM project by providing DCC related experimental data to be used in improving the models implemented in NEPTUNE CFD and by executing validation calculations of the code together with VTT. A specific POOLEX experiment series with a thermally insulated blowdown pipe and small steam mass flux was carried out for the purposes of the NURESIM project. Due to thermal insulation there was no condensation on the blowdown pipe inner walls but only at the steam-water interface close to the pipe outlet.

2. POOLEX EXPERIMENT STB-31

The POOLEX test facility is an open cylindrical pool (5.0 m in height and 2.4 m in diameter) modelling the condensation pool of a BWR. The earlier steam discharge experiments with the facility were considered too challenging as initial validation cases due to very rapid direct contact condensation phenomena and unknown amount of condensation on the pipe walls. Therefore, it was decided to carry out an experiment series aimed at producing data of more stable nature. For these experiments the vertical blowdown pipe (inner diameter 214.1 mm) was thermally insulated to prevent condensation on the pipe inner wall. The nearby PACTEL test facility was used as a steam source. Figure 1 presents the POOLEX test facility and the locations of the steam line measurements. Figure 2 shows the measurements in the pool and Figure 3 in the vicinity of the pipe mouth.
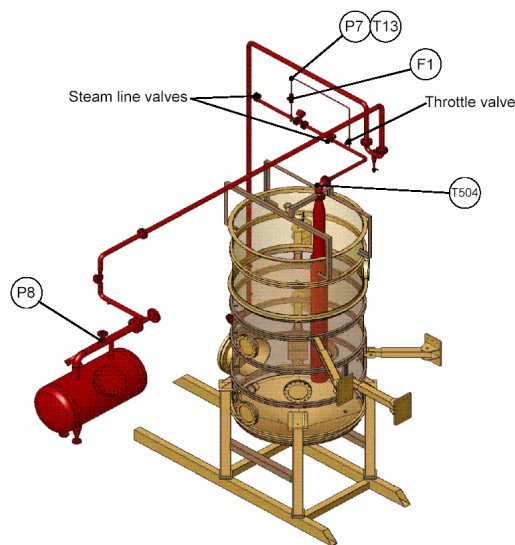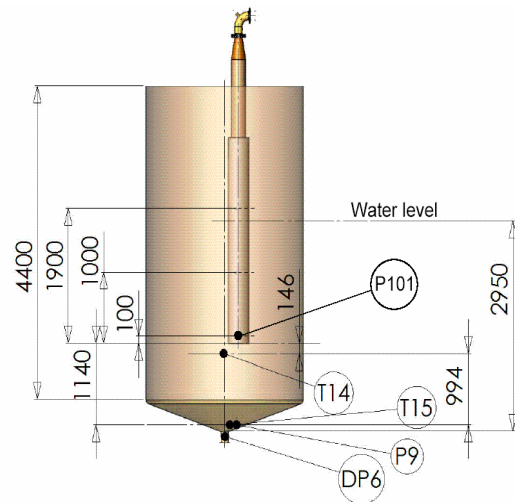

Fig 1: Test pool and steam line.
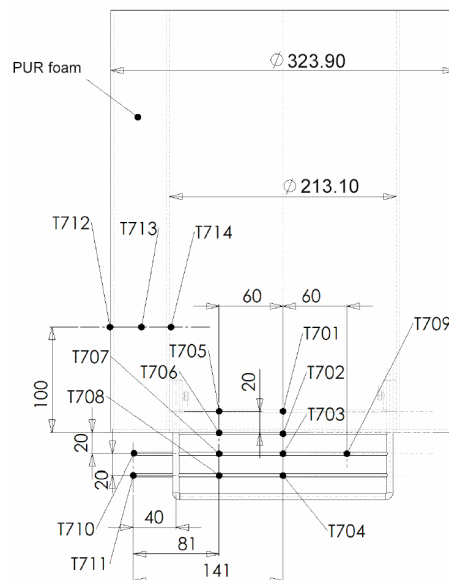
Fig 2: Instrumentation in the pool.

Fig 3: Thermocouples at the blowdown pipe outlet.

One experiment (labelled as STB-31) of the series was selected for the validation of NEPTUNE CFD condensation models. Before starting the measurements the pool was filled with isothermal water (32 °C) to a level of 2.95 m i.e. the total volume of water was approximately 12 m^3 and the blowdown pipe was submerged by 1.81 m. The duration of the experiment was about 6000 s. The steam mass

flow rate (0.5…1.5 g/s) was controlled along the experiment to prevent steam bubble formation and to keep the steam-water interface as close as possible to the pipe outlet. Several quasi-steady intervals suitable for the validation of direct contact condensation models can be found from the experiment data.

For the CFD simulations, a 300 s period (from 2040 s to 2340 s) from the STB-31 experiment was selected. Pressure in the blowdown pipe was almost constant (1.186 bar) during the selected period, and the time average value of mass flow rate in this period is 1.0594 g/s. These values are used in most of the simulations. The mass flow rate value corresponds also to intermediate conditions within the period, because, the mass flow rate is slowly decreasing linearly in time. This slight decrease in mass flow rate occurs due to decreasing condensation rate caused both by water heat up near the steam-water interface and by air layer accumulation to the steam-water interface. This air layer develops from dissolved gas that is released from the coolant during the blowdown. An effort to evaluate the amount of non-condensable gas in the vicinity of the steam-water interface during the selected period of the experiment was carried out. On the basis of air and steam partial pressures derived from measured temperatures and total pressure at the mouth of the pipe, the following bounding estimates were produced. Between the measurement inaccuracies, the lower limit for the height of the air layer can be 0.8 mm, the upper possible limit 30 mm, and the expected height of the layer 5 mm. Without the worst measurement inaccuracies in the mass flow rate, the layer height would be bounded between 2 and 6 mm. The concentration of non-condensable gas is assumed to decrease logarithmically within the layer with increasing elevation. An air layer would have a significant suppressing impact on DCC. In Figure 4, the temperature values at the pipe mouth (or discharge) and in the pipe are presented concerning the selected period. As the steam-water interface is very steadily at the mouth of the pipe, these values are mainly steam temperatures.
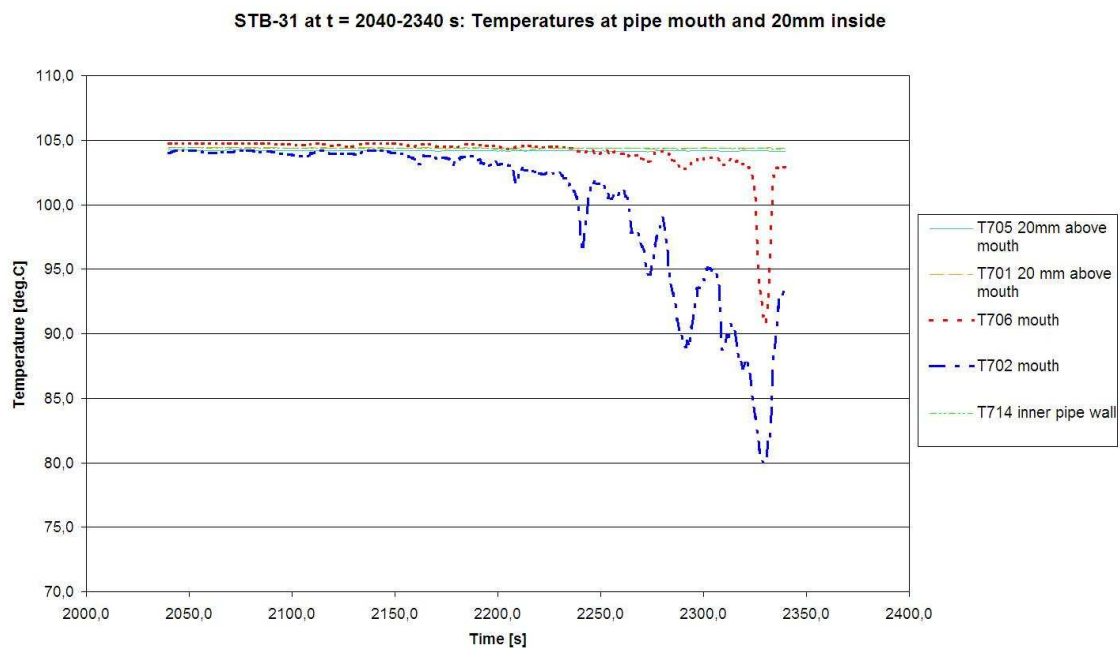

Fig 4: Temperatures at the pipe mouth, 20 mm above and at the inner wall.

Water below the blowdown pipe was heated up by condensing steam. This warmer water then rose towards the pool surface along the blowdown pipe outer wall due to buoyancy forces. Regarding temperatures outside the pipe (in the pool side), 30 °C for water and 104.3 °C for steam were selected to be used as initial values in the CFD-simulations.

3

3. PHYSICAL MODELS

The most relevant equations solved by NEPTUNE CFD that can be influenced by condensation are presented next. The equations are presented in Cartesian form, to simplify the presentation and to follow NEPTUNE CFD V1.0 Manual of Laviéville J. et al. (2006).

The multi-field mass balance equation for each field k is written:

$$\frac{\partial}{\partial t}\left(\alpha_k \rho_k\right) + \frac{\partial}{\partial x_i}\left(\alpha_k \rho_k U_{k,i}\right) = \Gamma_k \, , \qquad (1)$$

where α_k is volume fraction, ρ_k is density and U_k is mean velocity of phase k. Γ_k is the interfacial mass transfer rate on phase k. Γ_k is the sum of all other phase contributions.

The momentum equations are not presented here, because the effect of mass transfer is considered negligible in the practical form of the equations. The "non-conservative" form of energy equation reads

$$\rho_k \frac{\partial H_k}{\partial t} - H_k \frac{1}{\alpha_k} \frac{\partial}{\partial x_j}\left(\alpha_k \rho_k U_{k,j}\right) + \frac{1}{\alpha_k} \frac{\partial}{\partial x_j}\left(\alpha_k \rho_k H_k U_{k,j}\right) =$$

$$-\frac{1}{\alpha_k} \frac{\partial}{\partial x_j}\left(\alpha_k Q_{k,j}\right) + \frac{\partial P}{\partial t} + \rho_k U_{k,i} g_i + \frac{\varphi_{(wall \to k)}}{\alpha_k} \qquad (2)$$

$$+ \frac{1}{\alpha_k} \sum_{p \neq k} \left[\Pi'_{(p \to k)} + \Gamma^c_{(p \to k)} H^\sigma_{(p \to k)}\right] - \frac{\Gamma_k H_k}{\alpha_k},$$

where H_k is total enthalpy, Q_k is conductive thermal flux, P is mean pressure, g is acceleration due to gravity, φ represents the heat exchanges with boundaries (i.e. the nucleate boiling model), $\Pi'_{(p \to k)}$ is the part of interfacial heat transfer rate independent of the mass transfer, and $\Gamma^c_{(p \to k)} H^\sigma_{(p \to k)}$ is the part related to mass transfer, $H^\sigma_{(p \to k)}$ is the jump in enthalpy associated with mass transfer from phase p to phase k, and $\Gamma^c_{(p \to k)}$ is the mass transfer rate contribution from phase p to phase k. For contributions $\Gamma^c_{(p \to k)}$, the following relation must be verified:

$$\Gamma^c_{(p \to k)} = -\frac{\Pi'_{(p \to k)} + \Pi'_{(k \to p)}}{H^\sigma_{(p \to k)} - H^\sigma_{(k \to p)}} \qquad (3)$$

In two-phase water/steam flows these notations can be simplified, so for example for water phase Eq. (3) reduces to:

$$\Gamma^c_1 = \frac{\Pi'^{w/s}_1 + \Pi'^{w/s}_2}{H_2 - H_1} \qquad (4)$$

In the absence of nucleate mass transfer, the last term and the mass transfer contribution in the previous term in Eq. (2) can be cancelled. In the case with saturated vapour, the $\Pi_2^{'w/s}$ contribution is negligible in Eq. (4). The heat transfer rate $\Pi_1^{'w/s}$ has to be determined by use of a suitable condensation model.

3.1 Heat transfer rate by Hughes-Duffey model

In the modified Hughes-Duffey model (Hughes 1991) for turbulent stratified flows the heat transfer rate to water phase has equation:

$$\Pi_1^{'w/s} = a_i \zeta_1 \left(T_{sat} - T_1\right), \qquad (5)$$

where $a_i = |\nabla \alpha_1|$ is the interfacial area of quality [1/m]. T_{sat} is the saturation temperature and T_1 is the temperature of water. The heat transfer coefficient ζ_1 is defined as

$$\zeta_1 = \frac{Nu\lambda_1}{L_t},$$ (6)

where λ_1 is thermal conductivity and L_t is characteristic length. According to Hughes-Duffey model, Nu is defined as

$$Nu = \frac{2}{\sqrt{\pi}} \mathrm{Re}_t \, \mathrm{Pr}^{1/2},$$ (7)

where Re_t is

$$\mathrm{Re}_t = \frac{L_t u_t}{\nu}.$$ (8)

The length and velocity scales are defined as

$$L_t = C_\mu \frac{k_1^{3/2}}{\varepsilon_1} \quad \text{and} \quad u_t = C_\mu^{1/4} k_1^{1/2}.$$ (9)

The formulation used in NEPTUNE CFD derives by the substitution of Eqs. (7)-(8) into (6) and by defining numerical limitations to u_t:

$$\zeta_1 = \frac{2}{\sqrt{\pi}} \frac{\lambda_1}{\mu_1} \rho_1 V_L^* \sqrt{\mathrm{Pr}},$$ (10)

where

$$V_L^* = \max(V_L, 0.01) \quad \text{and} \quad V_L = \min\left(|U_1|, C_\mu^{0.25} \sqrt{q_1^2}\right)$$ (11)

Here μ_1 is viscosity, λ_1 is thermal conductivity and $q_1^2 = k_1$ is turbulent kinetic energy of phase 1 (water). $C_\mu = 0.09$ from the definition of k-ε-model. Note also that L_t cancels. Because this is a model effective on the water-steam interface, there is an auxiliary model to handle residual droplets. This model activates when $\alpha_1 < 0.1$ and has simple return to saturation form:

$$\Pi_1'^{w/s} = \alpha_2 \frac{\rho_1 C_{p1}}{\tau_1} (T_{sat} - T_1), \text{ where } \tau_1 = 1$$ (12)

Laviéville J. et al. (2006)

3.2 Heat transfer rate using Lakehal et al's. (2008) model

In the model of Lakehal et al's. (2008) (see also Banerjee et al., 2004 and Lakehal 2007), Nu takes the form:

$$Nu = Bf\left[\mathrm{Re}_t^m\right] \mathrm{Re}_t \, \mathrm{Pr}^{1/2}$$ (13)

In this expression, B is a model constant (i.e. B = 0.35 for Pr = 1 and 0.45 for Pr >> 1), and the so-called surface-divergence function $f\left[\mathrm{Re}_t^m\right]$ takes the following form

$$f\left[\mathrm{Re}_t^m\right] = \left[0.3\left(2.83\,\mathrm{Re}_t^{3/4} - 2.14\,\mathrm{Re}_t^{2/3}\right)\right]^{1/4} \mathrm{Re}_t^{-1/2}$$ (14)

The turbulent Reynolds number in this model is defined as

$$\mathrm{Re}_t = \frac{k_l^2}{\nu\varepsilon_l}$$ (15)

Otherwise, the heat transfer coefficient is the same as in Eq. (6). As the length scale L_t does not cancel in this model, it is calculated using Eq. (8), using:

$$L_t = \frac{\mathrm{Re}_t \nu}{u} = \frac{\mathrm{Re}_t \nu}{V_L}$$ (16)

Where V_L is the integral velocity scale, also defined as in the Hughes-Duffey model,

$$V_L = \min\left(|U_1|, C_\mu^{0.25} \sqrt{k_l}\right)$$ (17)

4. COMPUTATIONAL GRIDS

Two versions of 2D axisymmetric grids were generated for the simulations. The first grid contained 32450 hexahedral cells. The mesh was made more refined at the pipe tip region (Figure 5). Another grid containing 30650 cells was also employed; this was homogenous in the axial direction and refined in the radial direction towards the pipe wall. This grid was coarser than the first one in the pool area, but denser inside the pipe. These grids were made by rotating a 2D-grid around the axis of rotation to create an angular dimension of thickness of a single cell. Prismatic cells were avoided by truncating the geometry "microscopically" along the axis of rotation.
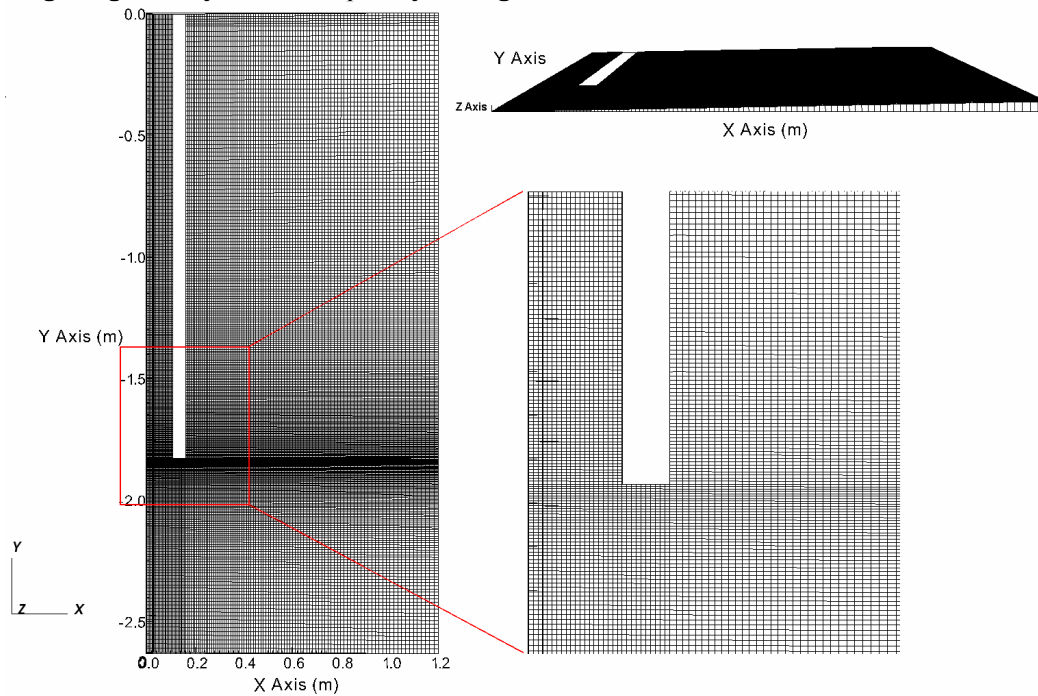

Fig 5: The 2D-axisymmetric calculation grid.

The radius of the domain was set to 1.2 m, which was the mean radius from the centre of the blowdown pipe to the wall of the condensation pool. (In the POOLEX test facility the pipe was not exactly at the centre of the pool). The height of the domain was set to 2.63 m. By using this height, the initial surface of water could be set on the upper edge of the domain. The lower conical part of the pool was truncated at 0.8 m from the mouth of the pipe. These simplifications should have negligible effect on the results. With these simplifications, it was possible to avoid the use of free air surface at the top of the pool and the conical geometry at the bottom of the pool.

A couple of full 3D-grids were generated also. The larger one of these contains 116268 cells. The same radial and vertical dimensions as in the 2D-axisymmetry case were used.

5. INITIAL AND BOUNDARY CONDITIONS, SIMULATION DETAILS

Most of the CFD simulation cases of STB-31 were initialized to conditions where the steam-water interface was exactly at the tip of the blowdown pipe. Thus, the initial volume fraction of steam was one in the pipe, and the volume fraction of water liquid was one outside the pipe. The pressure in the pipe was initialized to 1.186 bar and the pressure on the water surface of the pool was set to 1.0132 bar. The pressure in the liquid volume was initialized using hydrostatic pressure. The temperature in the liquid occupied region was initialized to 30 ºC and in the vapour region to 104.3 ºC. The initial density of water liquid was 995.6 kg/m^3 and the initial density of steam 0.689 kg/m^3. The initial specific heat capacities of water and steam were 4180 J/kg and 2095 J/kg, respectively. The initial viscosities of water and steam were 7.96e-4 Pas and 1.24e-5 Pas.

6

Two types of inlet boundary conditions were used. In most of the Hughes-Duffey simulations, velocity (or mass flow in 3D cases) boundary condition was used for steam inlet. Based on a quasi-steady period in the experiment an inlet velocity of 0.043 m/s was usually selected for steam. This corresponds to a mass flow rate of 1.0594 g/s. In the later simulations, where Hughes-Duffey and Lakehal et al. (2008) were compared, a pressure boundary condition of 1.186 bar was used instead.

The CATHARE steam tables built in NEPTUNE CFD, have been enabled and enthalpy scalars have been initialized by using initial temperature, pressure or H_{sat}. The standard k-epsilon turbulence model has been used for the water liquid phase and laminar assumption for the steam phase (although with momentum interaction with liquid phase being enabled). The drag model for separated phases has been applied to the steam phase.

The condensation model (Hughes-Duffey, Hughes-Duffey with modifications or Lakehal) was activated for the water phase. Because the steam phase was in saturation conditions, no heat transfer or condensation models were activated for that phase.

The simulations were computed using adaptive time-stepping. Typically, the initial time-step was set to 0.001 seconds.

6. RESULTS AND DISCUSSIONS

6.1 Cases with velocity inlet boundary condition

In Hughes-Duffey simulations with velocity inlet boundary condition, steady or long duration quasi-steady steam volume could not be maintained in the blowdown pipe by using measured velocity values or even slightly higher ones. More promising results were obtained after modification of the problematic auxiliary parameters in the original Hughes-Duffey distribution of NEPTUNE CFD. Figure 6 presents the effects of these modifications at 0.51 s of real time with the help of three cases.
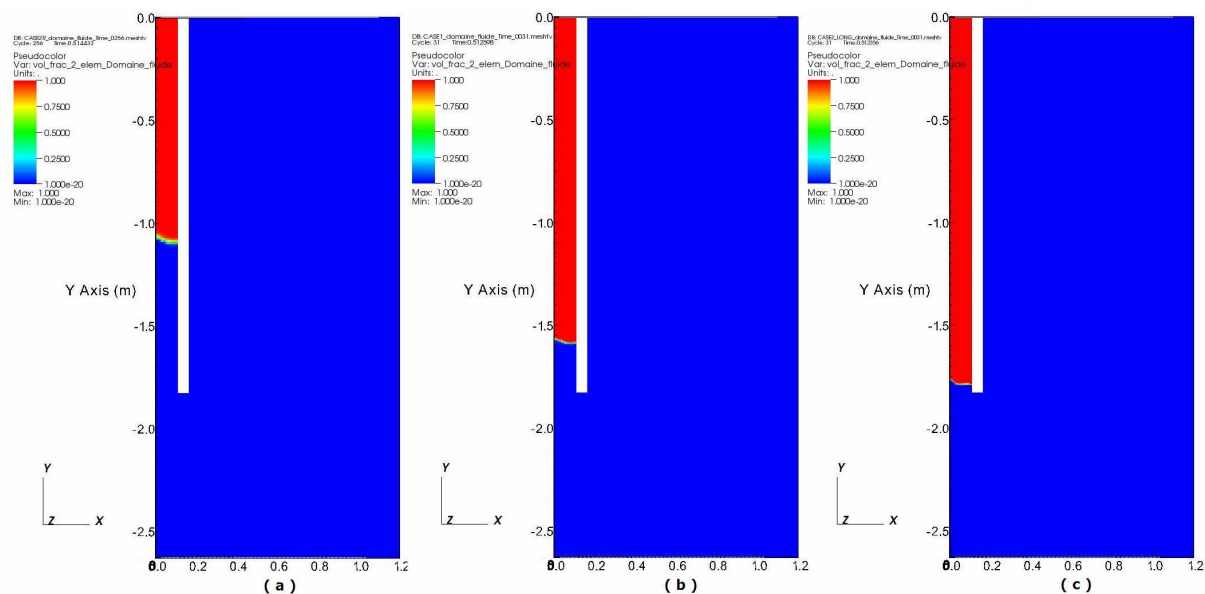

Fig 6: Steam volume development at t ≈ 0.51 s in standard simulation cases of the STB-31 experiment using the original and two different modifications of the stratified flow condensation model of NEPTUNE CFD. (a) the original model, (b) the case where V_L^* truncation criterion is decreased to 0.0001, and (c) the case where residual droplet auxiliary model is disabled in addition to the changes introduced in case (b).

As one can see from Figure 6, the above mentioned modifications are not sufficient to solve the problem of too high condensation rate and to maintain steady or quasi-steady steam volume in the pipe. The situation in Fig 6(c) (later called Hughes-Duffey modification 'c') might seem promising, but the steam volume is collapsing rapidly also in that case. Significantly longer simulation periods might be needed to prove that the steam-water interface starts to return towards the pipe outlet after sufficient water surface heat up.

Figure 7 presents the development of steam inventory in the blowdown pipe, the highest heat transfer coefficient found in the domain and the corresponding liquid phase turbulence kinetic energy value. Modification 'c' of the Hughes-Duffey condensation model was used in these simulations.
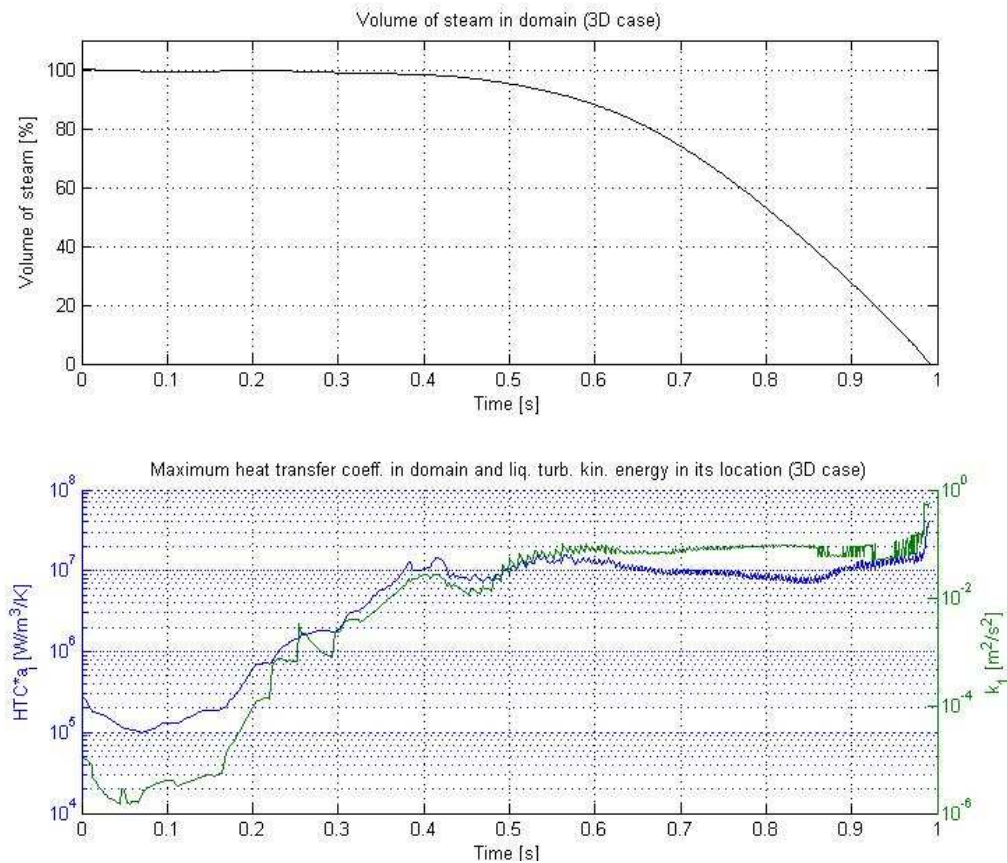

Fig 7: Vapour inventory in the blowdown pipe (upper figure) and maximum heat transfer coefficient in the domain with liquid phase turbulence kinetic energy at its location (lower figure). A 3D-simulation of the STB-31 experiment using modification 'c' of the Hughes-Duffey condensation model.

As can be seen from Figure 7, the liquid phase turbulence kinetic energy tends to dominate in the heat transfer coefficient of equations (9-11) if the limitation $\min(|U_1|, u_t)$ does not choose $|U_1|$ instead. In this case, it was observed that u_t is generally clearly smaller than $|U_1|$, and thus it determines the condensation rate as it should to do in normal conditions.

The DCC model of Lakehal et al.(2008) produced significantly lower condensation rates. In Figure 8, steam inventory and the maximum heat transfer coefficient are presented for the Hughes-Duffey modification 'c' and for the DCC model of Lakehal et al. (2008). As can be seen, the condensation rate is clearly smaller in the case of Lakehal et al. model and the maximum value of heat transfer coefficient is at least one order of magnitude smaller than in the Hughes-Duffey case.
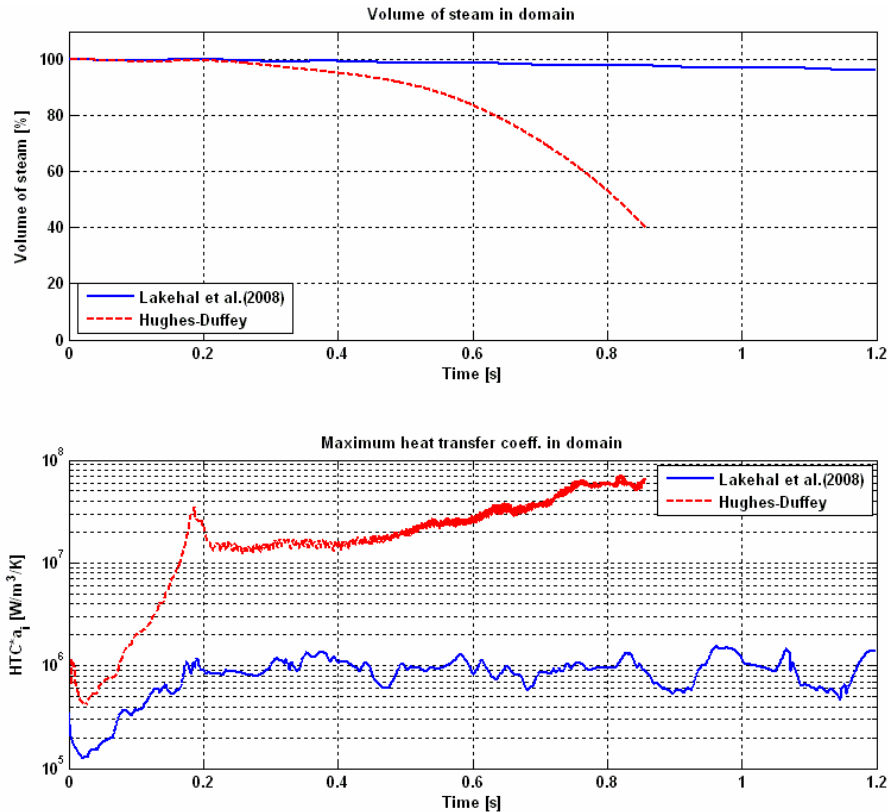
8

Fig 8: Vapour inventory in the blowdown pipe (upper figure) and maximum heat transfer coefficient in the domain (lower figure). 2D-axisymmetric simulations of the STB-31 experiment using modification 'c' of the Hughes-Duffey condensation model and the condensation model of Lakehal et al. (2008).

6.2 Results of simulation cases with pressure inlet boundary condition

A number of simulations were calculated using pressure boundary condition at the blowdown pipe inlet. Using pressure boundary condition, comparison of the condensation rates become easier, because the pressure boundary condition forces the steam inventory in the pipe to similar pressure equilibrium in every simulation case. In the chosen quasi-steady period of the STB-31 experiment the pressure in the blowdown pipe was steadily at 1.186 bar. Longer simulation periods are possible as well, because the steam inventory cannot collapse due to excessive condensation rates.

Figure 9 presents the steam inventory state in the blowdown pipe and the maximum heat transfer coefficient in the Hughes-Duffey 'c' and Lakehal et al., (2008) DCC-model simulation cases with the pressure inlet boundary condition. As can be seen from Figure 9, the steam inventory is almost maintained at 97 % of the original volume and thus the water-steam interface stays near the pipe outlet and oscillates slightly with decreasing amplitude. Concerning the heat transfer coefficients, the maximum value in the Lakehal et al. case is at least one order of magnitude smaller than in the Hughes-Duffey case, just as it was in the velocity inlet boundary condition cases.

The steam mass flow rates of the pressure inlet simulation cases are shown in Figure 10. As the heat transfer coefficients and Figure 10 indicate, the values of mass flow rates in the cases of the Hughes-Duffey condensation model are almost an order of magnitude higher compared to the values in the experiment and in the simulations with the Lakehal et al. model. The condensation rate also fluctuates rapidly in the Hughes-Duffey cases and the simulations do not reach convergence as easily as in Lakehal et al. cases.
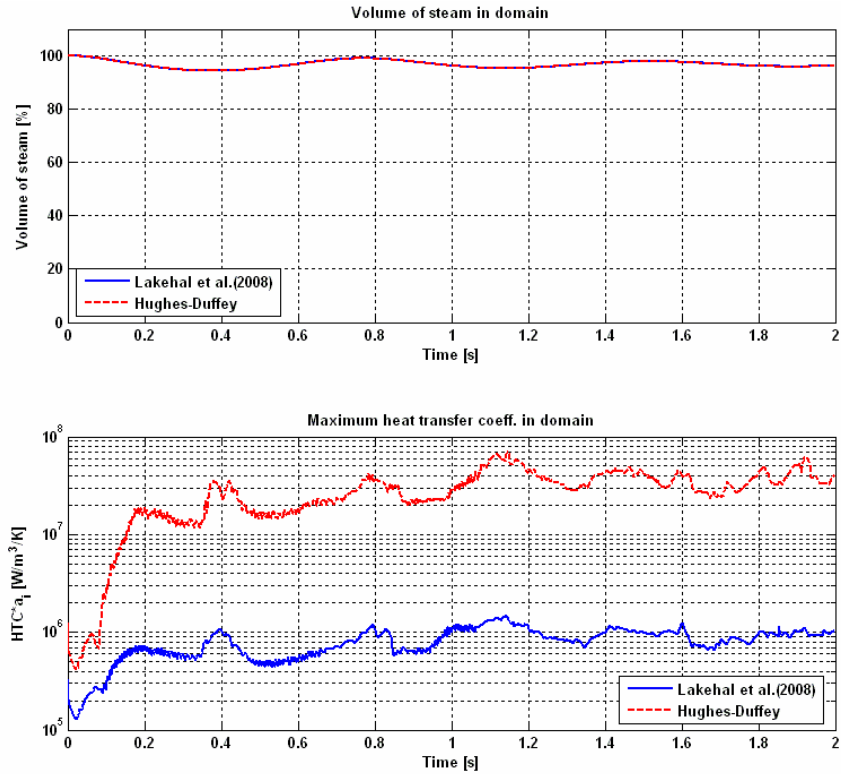
Fig. 9: Vapour inventory in the blowdown pipe and maximum heat transfer coefficient in simulations where the pressure inlet boundary (1.186 bar) is used. 2D-axisymmetric simulations of the STB-31 experiment using Lakehal et al.(2008) and Hughes-Duffey mod. 'c' condensation models.
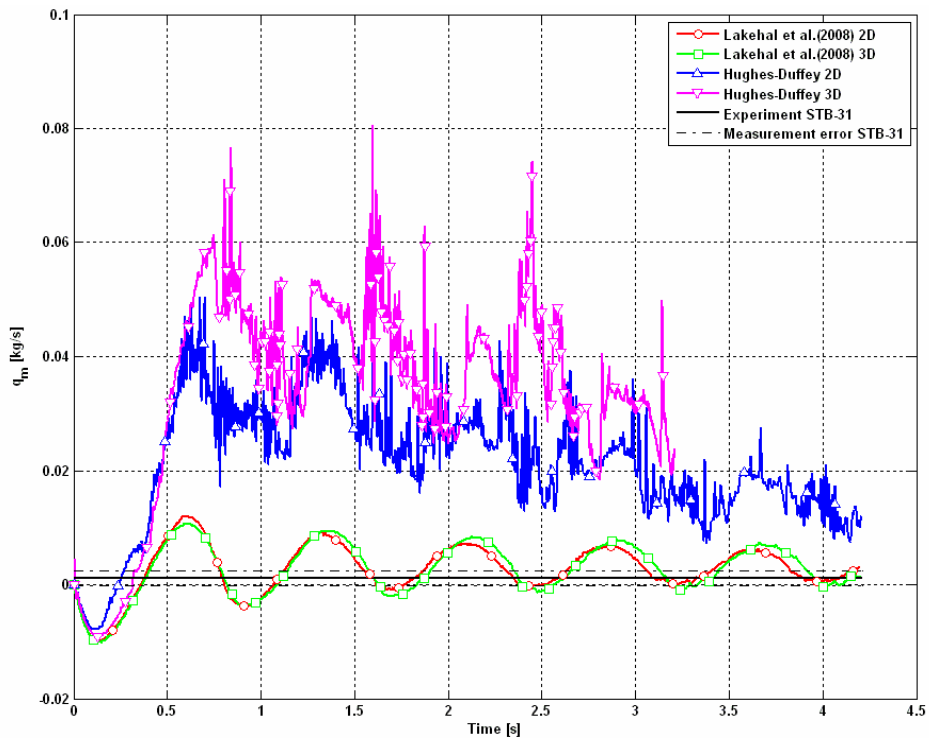

Fig. 10: Vapour mass flow rates recorded next to the blowdown pipe inlet in simulations where the pressure inlet boundary (1.186 bar) is used. Results of 2D-axisymmetric and 3D-simulations using Lakehal et al.(2008) and Hughes-Duffey mod. 'c' condensation models compared to the quasi-steady mass flow rate in STB-31.

10

As in the previous cases of the velocity inlet boundary condition, the liquid phase turbulence kinetic energy dominates in the heat transfer coefficient in the Hughes-Duffey model, if the limitation $\min(|U_l|, u_t)$ does not choose $|U_l|$ instead. This limitation is used also in the Lakehal model implementation, but in that model the turbulence kinetic energy is not as dominant term. Figure 11 shows the values of $|U_l|$ and u_t in the pressure inlet cases. As Figure 11 shows, the $\min(|U_l|, u_t)$ limitation does not activate $|U_l|$ frequently, and thus u_t determines the velocity scale in these models.
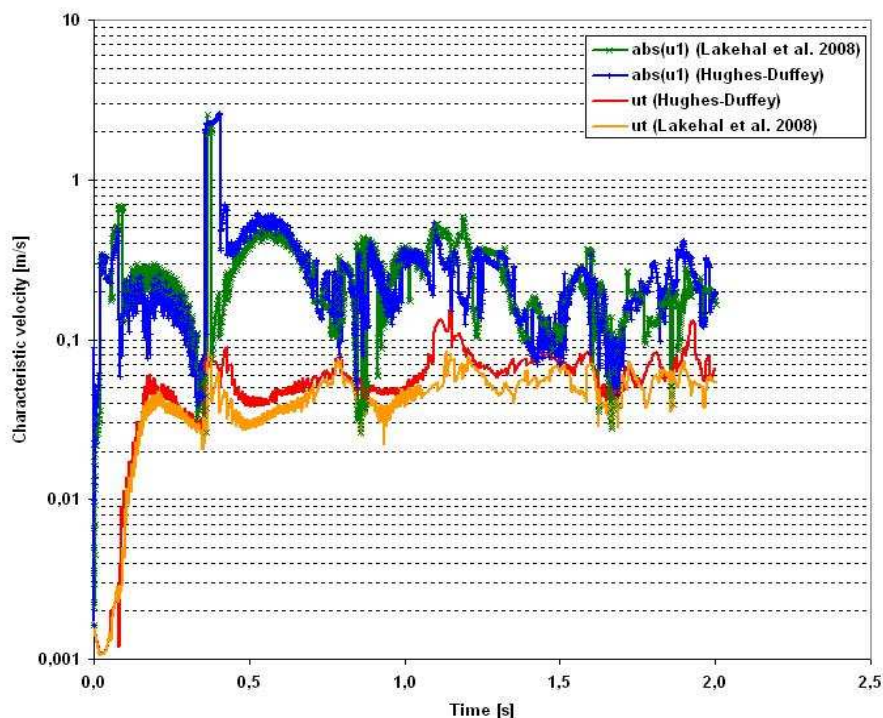

Fig. 11: Velocity magnitude and characteristic velocity related to turbulence kinetic energy in simulations where the pressure inlet boundary condition is used. Values are recorded from cells corresponding the location of maximum heat transfer coefficient.

6.3 Comparison with experiments

In the cases where the Hughes-Duffey condensation model was used, the condensation rates were at least one order of magnitude higher than in the STB-31 experiment. In the cases where the Lakehal et al. (2008) condensation model was used instead, the condensation rates were still slightly higher (in average) than in the experiment, but clearly in the same order of magnitude as in the experiment. However, some unknown amounts of non-condensables were present in the STB-31 experiment. Non-condensables have a suppressing effect on condensation. Therefore, high uncertainties still exist concerning the comparability of these DCC models with this single experiment. In this light, the final conclusions concerning applicability of these models should not be drawn.

7. FINAL REMARKS

7.1 Conclusions from this work

Lappeenranta University of Technology has carried out a specifically designed steam discharge experiment (STB-31) with the POOLEX test facility and made the measured data available to be used in the validation of the NEPTUNE CFD code developed within the EU/NURESIM project. The simulations indicated clearly higher condensation rates than in the experiment, when the Hughes-Duffey based stratified flow condensation model of NEPTUNE CFD was used. This overestimation was decreased remarkably by decreasing a numerical truncation parameter and by disabling the

residual droplet condensation auxiliary model. After these modifications, at least one order of magnitude over-estimation of the mass transfer rate still prevails. For comparison, the condensation model of Lakehal et al.(2008) was implemented into the code. This model is an adapted variant of the Banerjee et al. (2004) model for passive scalar transport across sheared turbulent streams. Using Lakehal's model, the condensation rates were significantly decreased to the same order of magnitude as in the experiment. The model has also been shown to be more stable than the previous one. One reason for this is probably the fact, that in the Lakehal et al. (2008) model the turbulence kinetic energy is damped by the turbulence dissipation rate whereas in the Hughes-Duffey model this tends to dominate the heat transfer coefficient.

High uncertainties exist concerning the comparability of these models with the STB-31 experiment, because the contribution of non-condensable air layer was not included. It is likely, that these condensation models would yield much lower condensation rates if this logarithmically concentrated 1-6 mm thick layer of non-condensables had been be modelled. Concerning the implemented version of the Lakehal et al. (2008) model, it would have been more preferable to use the inner scaling version of the model, because the steam-water interface in the STB-31 case was not significantly turbulent. Now, the outer scaling (surface divergence theory) version was used, because its implementation into NEPTUNE CFD was simple and possible to be done according to the schedule of the project.

7.2 Recommendations

Further validation work and comparisons of the condensation models discussed here is needed. Generally speaking, further validation and development of all condensation related models are still recommended. For example, concerning the STB-31 experiment, inner scaling version of the Lakehal et al. (2008) model would be tested. In order to increase the reliability of DCC validation in future, it will be necessary to obtain high grade data of experiments where the amount of non-condensable gases is absolutely negligible. As the knowledge of DCC has a great importance in any NPP concepts where the emergency steam suppression could be needed (i.e. BWRs), research work on this phenomenon and its modelling should be continued.

REFERENCES

S. Banerjee, M. Fulgosi, D. Lakehal, "Surface Divergence Models between Turbulent Streams", International Journal of Multiphase Flow, 30(7/8), pp. 963-977, (2004).

E.D. Hughes, R.B. Duffey, "Direct Contact Condensation and Momentum Transfer in Turbulent Separated Flows", International Journal of Multiphase Flow, 17(5), pp. 599-619, (1991).

D. Lakehal, "Direct Numerical Simulation of Condensing Stratified Two-Phase Flow", 6th Euratom Framework Program NURESIM Deliverable D2.1.7.2, (2007), European Commission, 6th Euratom Framework Programme 2005-2008, Integrated Project (IP): NURESIM Nuclear Reactor Simulations Sub-Project 2: Thermal Hydraulics, European Commission, 2007.

D. Lakehal, M. Fulgosi, G. Yadigaroglu, "DNS of a Condensing Stratified Steam-Water Flow", ASME J. Heat Transfer, 130, 021501-10, (2008).

J. Laviéville, E. Quémérais, S. Mimouni, M. Boucker, N. Méchitoua, "NEPTUNE CFD V1.0 theory manual", Copyright EDF-2006.

V. Tanskanen, M. Puustinen, J. Laine, "Validation of NURESIM-CFD against POOLEX condensation pool experiment", 6th Euratom Framework Program NURESIM, Deliverable D2.1.15.2b, (2008)., p. 24, European Commission, 6th Euratom Framework Programme 2005-2008, Integrated Project (IP): NURESIM Nuclear Reactor Simulations Sub-Project 2: Thermal Hydraulics, European Commission, 2008.